

DESY 02-025
 KEK-CP-123
 BI-TP 2002/03
 LMU-01/02
 March 2002

hep-ph/0203220
 ISSN 0418-9833

One-loop corrections to the process $e^+e^- \rightarrow t\bar{t}$ including hard bremsstrahlung ^{*} [†]

J. Fleischer^{1†} J. Fujimoto², T. Ishikawa², A. Leike³, T. Riemann⁴,
 Y. Shimizu² and A. Werthenbach⁴

¹ Fakultät f. Physik, Universität Bielefeld, 33615 Bielefeld, Germany

² High Energy Accelerator Research Org. (KEK), Oho 1-1, Tsukuba, Ibaraki 305-0801, Japan

³ Sektion Physik der Universität München, 80333 München, Germany

⁴ Deutsches Elektronen-Synchrotron, DESY Zeuthen, 15738 Zeuthen, Germany

ABSTRACT

Radiative corrections to the process $e^+e^- \rightarrow t\bar{t}$ are calculated in one-loop approximation of the Standard Model. There exist results from several groups [1], [2, 3], [4, 5], [6]. This talk provides further comparisons of the complete electroweak contributions, including hard bremsstrahlung. The excellent final agreement of the different groups allows to continue by working on a code for an event generator for TESLA and an extension to $e^+e^- \rightarrow 6$ fermions.

^{*} Talk presented by J. Fleischer.

[†] Work supported in part by the European Community's Human Potential Programme under contract HPRN-CT-2000-00149 Physics at Colliders.

[‡]E-mails: fl@physik.uni-bielefeld.de, Junpei.FUJIMOTO@th.u-psud.fr, tadashi.ishikawa@kek.jp,
 leike@theorie.physik.uni-muenchen.de, Tord.Riemann@desy.de, shimiz@suchi.kek.jp,
 Anja.Werthenbach@desy.de

The process $e^+e^- \rightarrow t\bar{t}$ is one of the most prominent and important processes to be measured at TESLA in order to find possible deviations from the Standard Model and thus ‘New Physics’. Several groups have had results for the one-loop corrections, but comparisons were not performed in all details. In order to provide finally an event generator for the evaluation of experimental data, such comparisons are mandatory. The **topfit** collaboration [6] having compared before the QED and weak corrections including soft photon contributions with [2,3], see Ref. [7], we are now also comparing the hard bremsstrahlung. This calculation has been performed before by the GRACE group [8] as well and in the present comparison we find excellent agreement between the results of our two groups, which means that the technical precision of the one-loop approach is completely tested. Thus we have been able to collect all the necessary codes to go on to more elaborate calculations, like e.g. inclusion of higher order corrections and a pole approximation of the process $e^+e^- \rightarrow 6$ fermions, see e.g. [9,10].

We define the following four-momenta and invariants: $k_{1,2}$ for $e^{-,+}$, $p_{1,2}$ for t, \bar{t} , p for the photon γ , c.m. energy: $s = (k_1 + k_2)^2$, $s' := (p_1 + p_2)^2$ invariant mass of the top pair and $t = (k_1 - p_1)^2$.

In Refs. [2,3], the following basis was introduced for the decomposition of the scattering matrix element into amplitudes:

$$\begin{aligned} M_1^{\rho\kappa} &= [\bar{u}_t(p_1)\gamma^\mu\omega_\rho v_t(p_2)] [\bar{v}_e(k_2)\gamma_\mu\omega_\kappa u_e(k_1)] \\ M_2^{\rho\kappa} &= [\bar{u}_t(p_1)\not{k}_2\omega_\rho v_t(p_2)] [\bar{v}_e(k_2)\not{p}_1\omega_\kappa u_e(k_1)] \\ M_3^{\rho\kappa} &= [\bar{u}_t(p_1)\omega_\rho v_t(p_2)] [\bar{v}_e(k_2)\not{p}_1\omega_\kappa u_e(k_1)] \\ M_4^{\rho\kappa} &= [\bar{u}_t(p_1)\gamma^\mu\not{k}_2\omega_\rho v_t(p_2)] [\bar{v}_e(k_2)\gamma_\mu\omega_\kappa u_e(k_1)], \end{aligned}$$

where

$$\omega_\lambda = \frac{1 + \lambda\gamma_5}{2}, \lambda = \pm 1.$$

For $m_e = 0$ (as assumed here), only 6 independent amplitudes of the 16 introduced above remain: there exist relations like

$$\begin{aligned} M_4^{-+} &= -m_t (M_1^{++} + M_1^{-+}) + 2M_3^{-+} \\ M_2^{++} &= -m_t M_3^{-+} + \frac{1}{2} (m_t^2 M_1^{-+} + t M_1^{++}) \\ M_3^{++} &= M_3^{-+}. \end{aligned}$$

One crucial subject of our present comparison is the hard bremsstrahlung. Therefore we give an extensive account of the bremsstrahlung in general. The initial- and final-state bremsstrahlung are shown in Figs. 1,2. Special, often used invariants, are the following: Z_1 and Z_2 from the propagators of the electron and positron in the diagrams of the initial-state radiation,

$$\begin{aligned} Z_1 &= 2p \cdot k_1 = -[(k_1 - p)^2 - m_e^2] \\ Z_2 &= 2p \cdot k_2 = -[(p - k_2)^2 - m_e^2] \end{aligned}$$

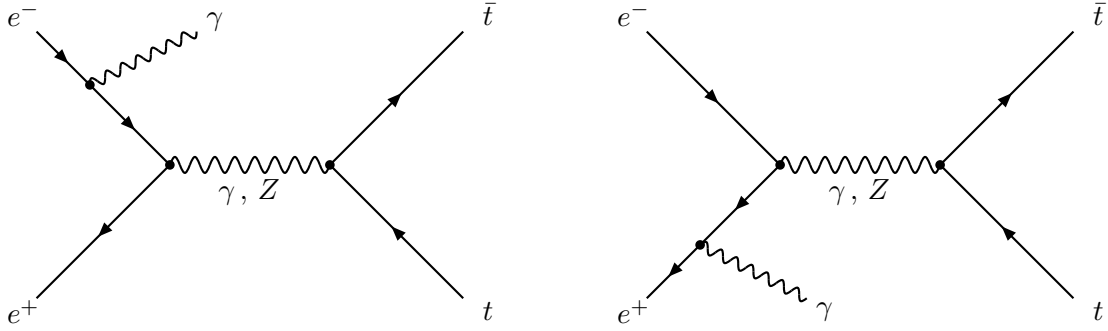


Figure 1: Feynman diagrams for initial-state radiation

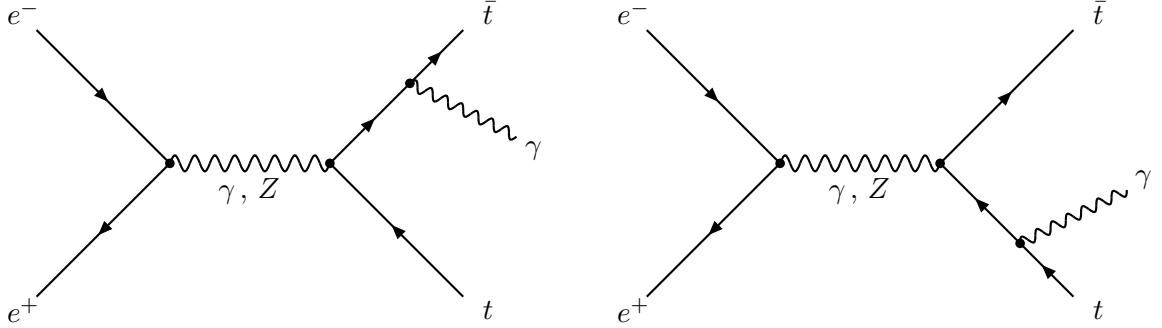


Figure 2: Feynman diagrams for final-state radiation

and similarly V_1 and V_2 from the propagators of the final top and anti-top of the final-state radiation,

$$V_1 = 2p \cdot p_1 = [(p + p_1)^2 - m_t^2]$$

$$V_2 = 2p \cdot p_2 = [(p + p_2)^2 - m_t^2].$$

The differential cross section of the bremsstrahlung reads:

$$d\sigma = \frac{(2\pi)^4}{2s} |M_{ini} + M_{fin}|^2 d\Phi_3,$$

where $d\Phi_3$ is the differential phase space of three outgoing particles (see below).

Of the one-loop vertex corrections we show the QED ones in Fig. 3. The mechanism of cancellation of the infrared (IR) soft photon divergences is as follows:

the interference between the Born and the initial state vertex diagram cancels the IR-divergences of

$$|M_{ini}|^2,$$

the interference between the Born and final state vertex diagram cancels the IR-divergences of

$$|M_{fin}|^2,$$

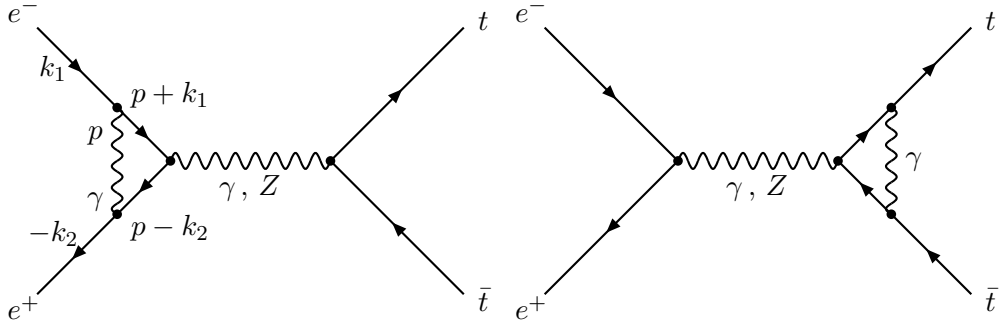


Figure 3: The photonic vertex corrections.

the interference between M_{ini} and M_{fin} is cancelled by box-diagrams ($\gamma\gamma$ and γZ in the s-channel).

The phase space of the process under consideration may be characterized by the following four independent kinematical variables:

- $s' := (p_1 + p_2)^2$ as invariant mass squared of the top pair,
- $\cos\theta$ as cosine of the scattering angle of \bar{t} with respect to the e^- beam axis in the c.m.s. .
- $\cos\theta_\gamma$ as cosine of the polar angle between the three-momenta of \bar{t} and the photon in the c.m.s., which is related to V_2 via an algebraic relation.
- φ_γ as azimuthal angle of the photon in the rest frame of (\bar{t}, γ) (z -axis defined by \vec{p}_2 of \bar{t} in the c.m.s.).

The different angles of the phase space are shown in Fig. 4.

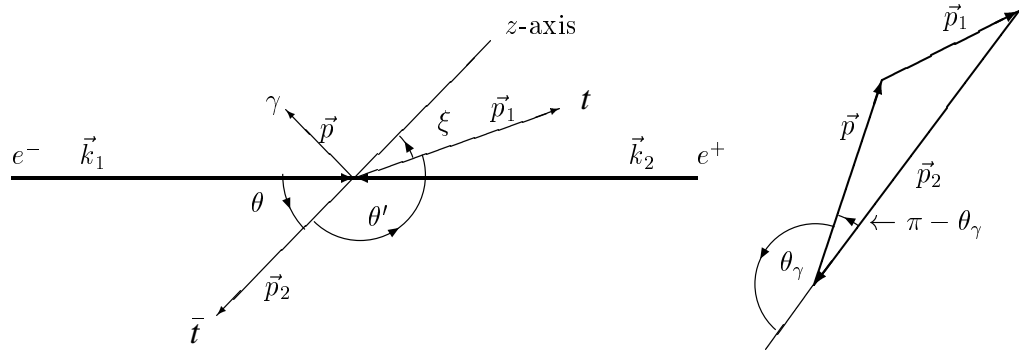


Figure 4: Angles of phase space and photon angle θ_γ .

Here ξ is the ‘acollinearity’ angle of the final fermions. $\xi = \pi$ means no constraint by collinearity, the requirement $\xi \ll 1$ restricts the kinematics to born-like events: only soft photons or photons collinear to one of the final fermions are allowed.

The integration over the phase space is reduced to an integration over the above four variables in the following manner: the two- and three-particle phase space elements are, respectively

$$d\Phi_2(1, 2) = \frac{d^3 \vec{p}_1}{2p_1^0} \frac{d^3 \vec{p}_2}{2p_2^0} \delta^4(p_{12} - p_1 - p_2)$$

and

$$d\Phi_3(1, 2, 3) = \frac{d^3 \vec{p}_1}{2p_1^0} \frac{d^3 \vec{p}_2}{2p_2^0} \frac{d^3 \vec{p}_3}{2p_3^0} \delta^4(p_{123} - p_{12} - p_3),$$

which can be written as

$$d\Phi_3(1, 2, 3) = d\Phi_2(1, 2) \times ds' \times d\Phi_2(12, 3).$$

This connection is presented graphically in Figs. 5 and 6.

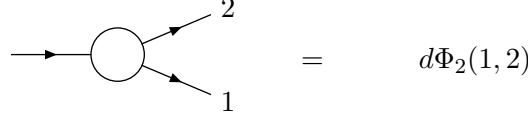


Figure 5: The 2-particle phase space.

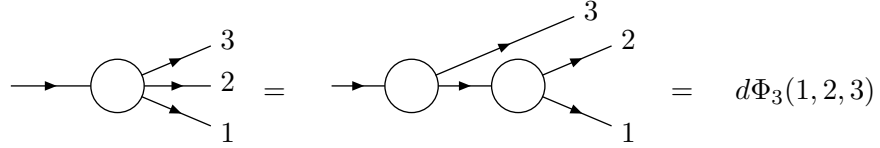


Figure 6: A sequential parametrization of the 3-particle phase space.

Thus the differential phase space volume $d\Phi^{(3)}$ finally is obtained as:

$$\begin{aligned} d\Phi_3 &= (2\pi)^4 \frac{d^3 \vec{p}_1}{(2\pi)^3 2p_1^0} \frac{d^3 \vec{p}_2}{(2\pi)^3 2p_2^0} \frac{d^3 \vec{p}}{(2\pi)^3 2p^0} \delta^4(\underbrace{k_1 + k_2}_{=k_{12}} - \underbrace{p_1 + p_2}_{=-p_{12}} - p) \\ &= (2\pi)^{-5} d^4 p_1 \delta(p_1^2 - m^2) d^4 p_2 \delta(p_2^2 - m^2) d^4 p \delta(p^2) \delta^4(k_{12} - p_{12} - p), \end{aligned}$$

which yields

$$\begin{aligned}
d\Phi_3(3) &= \frac{1}{(2\pi)^5} \frac{\pi}{16s} d\varphi_\gamma dV_2 ds' d\cos\theta \\
&= \frac{1}{2} \frac{s}{(4\pi)^4} d\varphi_\gamma d\left(\frac{V_2}{s}\right) d\left(\frac{s'}{s}\right) d\cos\theta \\
&= \frac{1}{2} \frac{s}{(4\pi)^4} d\varphi_\gamma dx dr d\cos\theta,
\end{aligned}$$

where the dimensionless variables

$$r \equiv \frac{s'}{s} \quad \text{and} \quad x \equiv \frac{V_2}{s}$$

have been introduced. With the cross-section:

$$d\sigma(2 \rightarrow 3) = \frac{(2\pi)^4}{2s} \times |\mathcal{M}|^2 \times d\Phi_3(3),$$

the integration can be performed analytically over the azimuthal photon angle φ_γ :

$$\varphi_\gamma \in [0; 2\pi].$$

There are different reasons not to consider only the full phase space but also parts of it. A real detector cannot see particles, which are too close to the beam pipe. This deficiency can be taken into account by a constraint to $\cos\theta$ (acceptance cut):

$$-c \leq \cos\theta \leq c.$$

Calling the photon energy E_γ , there is a simple relation between E_γ and r , $r = 1 - 2E_\gamma/\sqrt{s}$. To keep the photon energy larger than some cut ω , i.e. $E_\gamma > \omega$, one has to constrain

$$r \leq 1 - 2\omega/\sqrt{s} = r_\omega.$$

In some experiments, one wants to exclude events with hard photons, i.e. one demands $E_\gamma \leq E_{max}(\gamma)$. This cut translates into the constraint

$$r = 1 - 2E_\gamma/\sqrt{s} \geq 1 - 2E_{max}(\gamma)\sqrt{s} = r_\gamma.$$

In Fig.7 different acollinearity and photon energy cuts are shown.

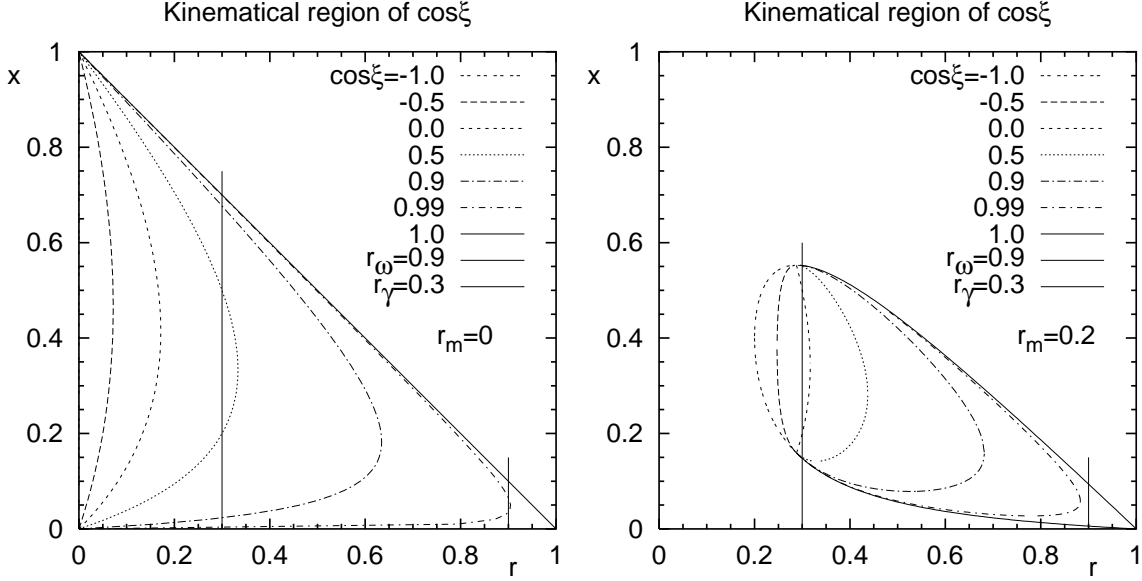


Figure 7: Phase space with acollinearity cut R_ξ : a. $r_m = \frac{4m_t^2}{s} = 0$ (zero top mass), b. $r_m = 0.2$ (non-zero top mass); $V_2/s \equiv x$.

In the following we present the results of the `topfit` and GRACE group and their comparison. We present total cross sections σ_{tot} and forward (F)-backward (B) asymmetries, which in an obvious notation reads $A_{FB} = \frac{\sigma_{FB}}{\sigma_{\text{tot}}}$ with $\sigma_{\text{tot}} = \sigma_F + \sigma_B$ and $\sigma_{FB} = \sigma_F - \sigma_B$. Further we separate QED and weak corrections: by QED we mean all IR-divergent diagrams (see Figs. 2,3 and boxes) including their counterterms plus born (0) and soft contributions. The Standard Model (SM) means QED plus weak, where the fermion contributions in the photon selfenergy and the charge renormalization are counted as ‘weak’. The notion ‘tot’ also means inclusion of hard photons (integrated over the whole phase space).

\sqrt{s}	σ_{tot}^0	A_{FB}^0	$\sigma_{\text{SM,tot}}$	$\sigma_{\text{SM,FB}}$	σ_{tot}	A_{FB}
500	T : 0.5122744	0.4146039	-0.1198972	-0.0855551	0.526337	0.362929
	G : 0.5122751	0.4146042	-0.1198973		0.526371	0.363140
1000	T : 0.1559185	0.5641706	-0.0683693	-0.0522582	0.171916	0.488869
	G : 0.1559187	0.5641710	-0.0683695		0.171931	0.488872

Table 1: Total cross sections (in pbarn) and forward-backward asymmetries. σ_{tot}^0 (Born) and $\sigma_{\text{SM,tot}}$ are ‘elastic’ and σ_{tot} includes hard photons, $\omega/\sqrt{s} = 0.00001$.

$\cos \theta$	ω/\sqrt{s}	$\left[\frac{d\sigma}{d \cos \theta} \right]_{\text{Born}}$	$\left[\frac{d\sigma}{d \cos \theta} \right]_{\text{QED}}$	$\left[\frac{d\sigma}{d \cos \theta} \right]_{\text{SM}}$	$\left[\frac{d\sigma}{d \cos \theta} \right]_{\text{tot}}$
-0.9	T : 0.1	0.108839194075	+0.098664253	+0.11408410	0.13144
	T : 0.00001	0.108839194075	-0.017474702	-0.002054858	0.13229
	G : 0.00001	0.108839194076		-0.002054859	0.13206(12)
-0.5	T : 0.1	0.142275069392	+0.12850790	+0.14308121	0.15973
	T : 0.00001	0.142275069392	-0.029702340	-0.015129038	0.16029
	G : 0.00001	0.142275069393		-0.015129039	0.16013(13)
+0.0	T : 0.1	0.225470464033	+0.20239167	+0.21718801	0.23638
	T : 0.00001	0.225470464033	-0.058010508	-0.043214169	0.23476
	G : 0.00001	0.225470464033		-0.043214168	0.23513(14)
+0.5	T : 0.1	0.354666470332	+0.31511723	+0.32933727	0.35651
	T : 0.00001	0.354666470332	-0.109721291	-0.095501257	0.35062
	G : 0.00001	0.354666470332		-0.095501252	0.35104(17)
+0.9	T : 0.1	0.491143715767	+0.43071437	+0.44290816	0.48796
	T : 0.00001	0.491143715767	-0.179672655	-0.16747886	0.47768
	G : 0.00001	0.491143715767		-0.16747886	0.47709(21)

Table 2: Various differential cross sections (see also text). The upper and lower numbers correspond to the topfit (T) and GRACE (G) approach, respectively, $\sqrt{s} = 500$ GeV.

$\cos \theta$	ω/\sqrt{s}	$\left[\frac{d\sigma}{d \cos \theta} \right]_{\text{Born}}$	$\left[\frac{d\sigma}{d \cos \theta} \right]_{\text{QED}}$	$\left[\frac{d\sigma}{d \cos \theta} \right]_{\text{SM}}$	$\left[\frac{d\sigma}{d \cos \theta} \right]_{\text{tot}}$
-0.9	T : 0.1	0.0227854232732	+0.020365844	+0.023101706	0.036334
	T : 0.00001	0.0227854232732	-0.004756230	-0.002020367	0.036461
	G : 0.00001	0.02278542327319		-0.002020369	0.036582(48)
-0.5	T : 0.1	0.0297821311031	+0.026741663	+0.028823021	0.038888
	T : 0.00001	0.0297821311031	-0.008561495	-0.006480137	0.039055
	G : 0.00001	0.0297821311031		-0.006480139	0.038965(42)
+0.0	T : 0.1	0.0611800674224	+0.054539344	+0.054950889	0.067789
	T : 0.00001	0.0611800674224	-0.021532420	-0.021120874	0.067801
	G : 0.00001	0.0611800674225		-0.021120874	0.068039(55)
+0.5	T : 0.1	0.117746949888	+0.10311626	+0.099416999	0.12095
	T : 0.00001	0.117746949888	-0.050123708	-0.053822973	0.12051
	G : 0.00001	0.117746949888		-0.053822964	0.12064(07)
+0.9	T : 0.1	0.181122097086	+0.15403823	+0.14426232	0.19355
	T : 0.00001	0.181122097086	-0.096682759	-0.10645866	0.19272
	G : 0.00001	0.181122097086		-0.10645866	0.19057(10)

Table 3: Same as Table 2, $\sqrt{s} = 1000$ GeV.

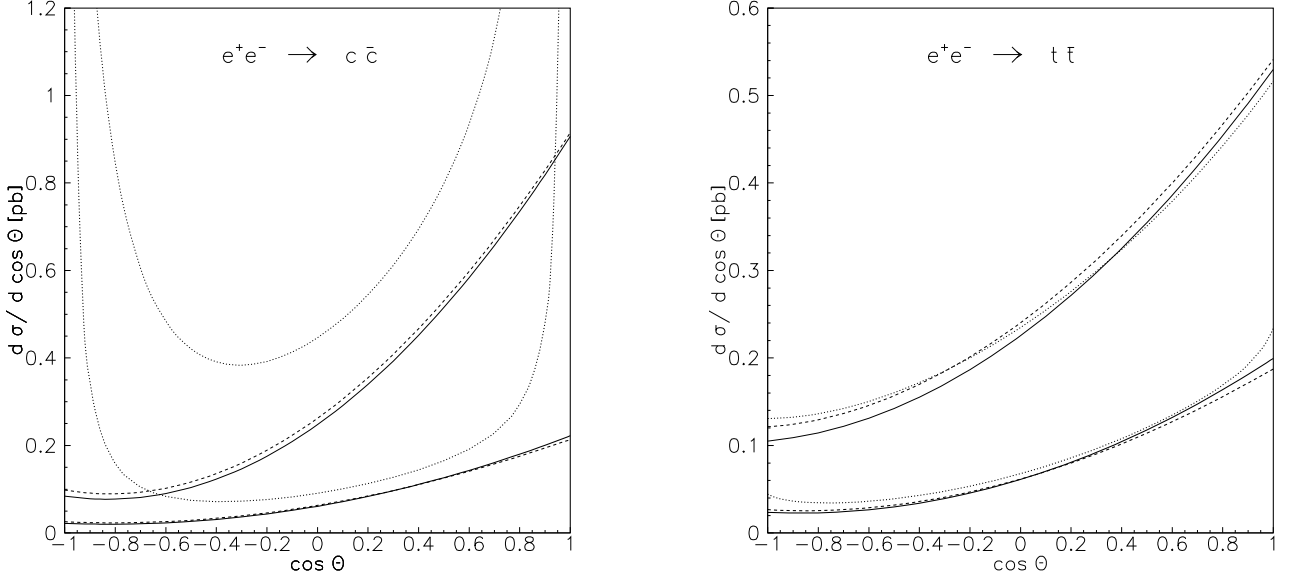


Figure 8: Differential hard photon cross sections $\frac{d\sigma}{d\cos\theta}$ of the processes $e^+e^- \rightarrow c\bar{c}$ and $e^+e^- \rightarrow t\bar{t}$. Solid, dashed and dotted lines stand for Born, weak and SM, respectively. Thin lines correspond to $\sqrt{s} = 500$ GeV and thick lines to $\sqrt{s} = 1000$ GeV.

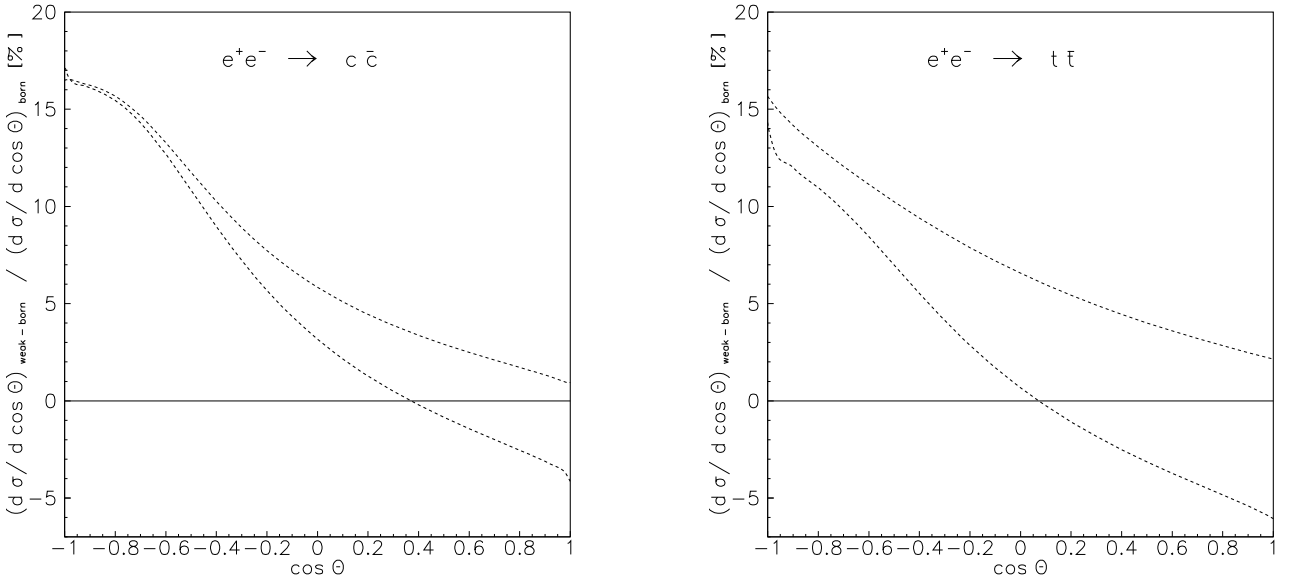


Figure 9: One-loop percentage corrections with respect to Born, corresponding to Fig.8. Thin lines stand for $\sqrt{s} = 500$ GeV and thick lines for $\sqrt{s} = 1000$ GeV.

In Table 1 the results are given for total cross sections for two energies and in Tables 2,3 for differential cross sections. If not stated otherwise, the parameter input is the same as in Ref. [7]. We see that the agreement is indeed excellent. As a general statement we can say, that the accuracy of the GRACE numbers for the non-hard-cross-sections is higher than shown while for the hard cross sections the same applies for the **topfit** numbers.

Concerning the ‘elastic’ entities in Table 1 we have in general an agreement of up to six decimals while in the hard ones the maximum error is contained in A_{FB} , which is 2×10^{-4} (.58 per mille). Concerning Table 2 we see that the differential Born cross sections agree up to 12 decimals. We also show the QED contributions for $\omega/\sqrt{s} = 0.1$ since they are slightly more precise than those shown in Ref. [7] due to a higher accuracy of the soft interference term. For practical applications this large soft photon cutoff is, however, not applicable. The agreement in Table 1 is least good for those results which include hard bremsstrahlung, but we have for $\omega/\sqrt{s} = 0.00001$ an agreement of 3 decimals. Presumably the errors given by the GRACE MC calculations are somewhat underestimated. Nevertheless the results of the GRACE group for σ_{tot} and A_{FB} in Table 1 are more precise than those for the differential cross sections in Table 2.

In Figs. 8 and 9 we present our results for the differential cross sections for $e^+e^- \rightarrow c\bar{c}$ and $e^+e^- \rightarrow t\bar{t}$ and the corresponding percentage corrections. For the $c\bar{c}$ channel we observe huge corrections in particular in forward and backward direction. These corrections are reduced drastically by cutting hard photons and are therefore not of real physical relevance. For $t\bar{t}$ production the mass serves as a cutoff.

Acknowledgement: One of us (J.F.) wants to thank DESY for extended kind hospitality.

References

- [1] J. Fujimoto and Y. Shimizu, *Mod. Phys. Lett.* **3A** (1988) 581.
- [2] W. Beenakker, S. van der Marck, and W. Hollik, *Nucl. Phys.* **B365** (1991) 24–78.
- [3] W. Hollik and C. Schappacher, *Nucl. Phys.* **B545** (1999) 98–140.
- [4] A. Andonov *et al.*, “Further study of the $e^+e^- \rightarrow f\bar{f}$ process with the aid of CalcPHEP system”, preprint (2002), [hep-ph/0202112](#).
- [5] D. Bardin, L. Kalinovskaya, and G. Nanava, “An electroweak library for the calculation of EWRC to $e^+e^- \rightarrow f\bar{f}$ within the CalcPHEP project”, Dubna preprint JINR E2–2000–292 (2000), [hep-ph/0012080](#), v.2 (12 Dec 2001).
- [6] J. Fleischer, A. Leike, T. Riemann, and A. Werthenbach, Fortran program **topfit.F** v.0.91 (06 March 2002), to be published.
- [7] J. Fleischer, T. Hahn, W. Hollik, T. Riemann, C. Schappacher, and A. Werthenbach, “Complete electroweak one-loop radiative corrections to top- pair production at TESLA: A comparison”, DESY preprint TESLA LC-TH-2002-002 (2002), [hep-ph/0202109](#).
- [8] F. Yuasa *et al.*, *Prog. Theor. Phys. Suppl.* **138** (2000) 18–23.
- [9] A. Aeppli, G. J. van Oldenborgh, and D. Wyler, *Nucl. Phys.* **B428** (1994) 126–146.
- [10] K. Kolodziej, “Top quark pair production and decay into 6 fermions at linear colliders”, preprint (2001), [hep-ph/0110063](#).

